

Manuscript Draft

Sally E. Claridge¹, Daniel M. Charytonowicz¹, & Adam A. Margolin^{1, 2}

¹ Department of Genetics and Genomic Sciences, Icahn Institute for Data Science and
Genomic Technology, Icahn School of Medicine at Mount Sinai, New York, NY
² Cancer Target Discovery and Development Network (Oregon Health and Science
University, Portland, OR), National Cancer Institute, National Institutes of Health

Author Note

Add complete departmental affiliations for each author here. Each new line herein
must be indented, like this line.

Enter author note here.

Correspondence concerning this article should be addressed to Adam A. Margolin,
Icahn School of Medicine at Mount Sinai, Department of Genetics and Genomic Sciences,
One Gustave L. Levy Place, Box 1498, New York, NY 10029. E-mail:
adam.margolin@mssm.edu

Abstract

Multiple high-throughput functional screens in cancer cell lines have generated large amounts of information on drug efficacy in a variety of genomic contexts and cancer lineages. Inconsistencies between datasets have led us to investigate whether these large-scale screens reproduce established clinical drug-gene associations and if genomic features particular to specific genes improve said reproducibility. We evaluated three large-scale, small-molecule drug screens and one CRISPR/Cas9 gene essentiality screen, all within the context of clinical interpretations derived from a new cancer variant annotation resource published by the Variant Interpretation for Cancer Consortium (VICC). We identified low levels of concordance between the three drug screen datasets and clinical drug-gene associations using mutation status, gene expression, and copy number as genomic indicators. Less than half of the clinical drug-gene cancer associations from the VICC resource were identified in these three drug screen datasets, suggesting a barrier to translating findings from these large-scale screens into the clinic.

Keywords: keywords

Word count: X

Manuscript Draft

Introduction

Cancer cell lines are a long-standing model for systematic testing of candidate therapeutics, beginning with the National Cancer Institute 60 (NCI60) assay from the late 1980s (M. C. Alley et al., 1988; R. H. Shoemaker, 2006; Stinson et al., 1992), which has been used to screen over 100,000 compounds as of 2010 (Holbeck, Collins, & Doroshow, 2010). Since then, numerous small-molecule and gene essentiality screens of various scales and study aims have been conducted in cell lines, from grouping drugs by therapeutic target similarity (Greshock et al., 2010) to screening only near-haploid cell lines to generate genome-level insights into gene essentiality (T. Wang et al., 2015) to broadly identifying cancer dependencies with large-scale screens in multiple cancer types (McDonald et al., 2017; J. M. McFarland et al., 2018; Meyers et al., 2017; Patel et al., 2017) or select lineages (Heiser et al., 2009; Marcotte et al., 2012; Patel et al., 2017). Despite their widespread use, cancer cell lines are known to have issues with inconsistent naming conventions and contamination (M. Yu et al., 2015), and some cell lines have been shown to vary widely at the genetic level and in response to drug treatment across strains (Ben-David et al., 2018). Additionally, comparisons between cancer cell lines and tumors indicate that cell lines have higher numbers of genomic aberrations (Domcke, Sinha, Levine, Sander, & Schultz, 2013; Mouradov et al., 2014; Neve et al., 2006) and tend to be hypermethylated (Paz et al., 2003; Varley et al., 2013), which could prove an impediment to translating cell line discoveries into the clinic.

There have also been debates over consistency between drug screen datasets, namely the Broad Institute’s and Novartis Institutes for Biomedical Research’s Cancer Cell Line Encyclopedia (CCLE) (J. Barretina et al., 2012; T. C. C. L. E. Consortium & Consortium, 2015) and the Genomics of Drug Sensitivity in Cancer (GDSC) from the Cancer Genome Project at the Wellcome Sanger Institute and the Center for Molecular Therapeutics at

Massachusetts General Hospital Cancer Center (Garnett et al., 2012; Yang et al., 2012). The GDSC has also been referred to as the Cancer Genome Project (CGP) and the Sanger dataset. Studies have shown that drug-gene interactions matched between CCLE and GDSC exhibited poor correlation and inconsistencies (Haibe-Kains et al., 2013; Jang, Neto, Guinney, Friend, & Margolin, 2014), prompting other groups to join the debate on how best correct for experimental and methodological variation between the original drug screens and subsequent computational analysis (T. C. C. L. E. Consortium & Consortium, 2015; Geeleher, Cox, & Huang, 2016; Geeleher, Gamazon, Seoighe, Cox, & Huang, 2016; Hatzis et al., 2014; Haverty et al., 2016; Safikhani et al., 2016, 2017).

The prevalence and importance of cancer cell lines in large-scale therapeutic research and the apparent inconsistencies between the GDSC and CCLE encouraged us to compare the results from these functional screens to clinical drug-gene associations. An outstanding question concerning studies based on cancer cell lines is whether these the cell line systems can accurately model tumor dynamics or recapitulate clinical cancer vulnerabilities, and many large-scale grants and clinical trials are fundamentally anchored by results from screens conducted in cancer cell lines. Thus, our goal was to evaluate how well these functional screens recapitulate known drug, gene, and tumor type associations that are currently used in clinical decision-making.

We derived our clinical associations from a new project conducted by the Variant Interpretation for Cancer Consortium (VICC; <https://cancervariants.org/>), a Driver Project for the Global Alliance for Genomics and Health (GA4GH) (The Global Alliance for Genomics and Health, 2016). The VICC has curated annotations of known cancer variants at varying levels of evidence from multiple resources (A. H. Wagner et al., 2018): the Precision Medicine Knowledgebase (L. Huang et al., 2016), MolecularMatch (<https://www.molecularmatch.com/index.html>), OncoKB (Chakravarty et al., 2017), Jackson Labs Clinical Knowledgebase (S. E. Patterson et al., 2016), Clinical Interpretations of Variance in Cancers (CIViC) (Griffith et al., 2017), and the Cancer

Genome Interpreter (CGI) (Tamborero et al., 2018). These harmonized variants are hosted on an ElasticSearch (Kibana v6.0) platform called Genotype to Phenotype (G2P, <https://search.cancervariants.org/#>*) that allows users to query and filter aggregated evidence from the various databases listed above as well as the GA4GH beacon service (<http://beacon-network.org/#/>), which yields access to genetic mutation data from over 200 datasets as of 2016 (The Global Alliance for Genomics and Health, 2016). For drug screen datasets, we focus on three well-known, large-scale drug projects: the CCLE and GDSC, which were mentioned above, and the Center for the Science of Therapeutics at the Broad Institute’s Cancer Therapeutics Response Portal (CTRP) dataset (Basu et al., 2013; M. G. Rees et al., 2016; B. Seashore-Ludlow et al., 2015). We also analyzed the results from a large-scale CRISPR/Cas9 screen conducted by the Broad Institute’s Cancer Dependency Map project (DepMap) using the Avana knockout library (Doench et al., 2016; Meyers et al., 2017), which will address whether gene essentiality screens via CRISPR yield results comparable to functional drug screens.

Results

Do small-molecule screens in cancer cell lines recapitulate clinical drug-gene associations?

G2P designed a set of standards for stratifying their database’s cancer variant interpretations, ranging from preclinical data at the low-evidence end (level D) to clinically actionable interpretations at the high-evidence end (level A). To test only these clinically actionable associations, we filtered the G2P dataset for only level-A G2P interpretations, of which there were 1,296 (see Methods). All compounds screened within the GDSC, CTRP, and CCLE datasets are considered “small molecules” and are respectively linked to Compound (CID) numbers used for indexing in the PubChem database (<https://pubchem.ncbi.nlm.nih.gov/>). As a result, non-small molecules, which include

Table 1

Level-A G2P interpretations excluded from analyses

Compound	CID	N_G2P	%
EGFR	SID160769799	1	0.25
pertuzumab	CHEMBL2007641	1	0.25
ipilimumab	CHEMBL1789844	2	0.50
cisplatin	CHEMBL2068237	3	0.75
pembrolizumab	CHEMBL3137343	3	0.75
nivolumab	CHEMBL2108738	4	1.00
trastuzumab	CHEMBL1201585	9	2.24
mAb	CHEMBL2109423	16	3.98
cetuximab	CHEMBL1201577	74	18.41
panitumumab	CHEMBL1201827	75	18.66
NA	NA	214	53.23

Note. N_G2P (%) = number of associated G2P interpretations, % is out of column total; mAb = monoclonal antibody; NA indicates G2P interpretation does not have an associated compound.

proteins and biologics (i.e. monoclonal antibodies), that had level-A G2P evidence could not be included in our comparisons. Thus, G2P interpretations for which the compound did not have a matching CID code were excluded from further analysis as were interpretations that did not have an associated compound, resulting in removal of 402 interpretations (Table 1). It should be noted that cisplatin, a small molecule, was excluded due to its being indexed with a ChEMBLdb identifier (<https://www.ebi.ac.uk/chembl/>), which we did not manually re-index to a CID to avoid accidental mischaracterization.

After filtering, 894 level-A G2P interpretations were carried forward in subsequent analyses, constituting 57 unique drugs and 34 unique genes in 88 distinct level-A combinations (*Figure 1A*). The number of level-A interpretations per drug ranged from 1 to 176 ($M = 15.68$, $SD = 34.63$), 1 to 264 ($M = 26.24$, $SD = 61.58$) per gene, and for each level-A drug-gene combination, the range was 1 to 103 ($M = 10.14$, $SD = 19.80$). These unique drugs, genes, and combinations are hereafter referred to as G2P drugs, G2P genes, and G2P associations. Filtering our screening datasets by these clinical criteria yields panels of potentially clinically relevant omic features. Of the 57 unique G2P drugs, 37 of them were screened in at least one of the drug screen datasets, 17 drugs were screened in at least two of the three datasets, and only 3 were screened in all three datasets. The remaining 20 un-screened G2P drugs suggests an incompleteness of these drug screens, though these projects frequently release new screening data that may include these drugs in future releases.

Using cell-line-specific point mutation annotations from the CCLE, we compared z-score-transformed area under the dose-response curve (AUC) distributions between mutant and wildtype cell lines for all G2P associations tested in the CCLE, CTRP, and GDSC drug screens. Of the 88 G2P associations, data was available for 9 associations in CCLE, 48 in CTRP, and 44 in GDSC. Controlling for a false discovery rate (FDR) $< 5\%$, CCLE yielded no significant correlations (Wilcoxon rank-sum tests, $p_k = 2.1^{-4}$), though the most significant G2P association was selumetinib-*KRAS* ($p_{adj} = 1.9^{-3}$). In CTRP,

AUC from 3 drug-gene associations correlated with the gene's mutation status ($p_k = 4.5^{-3}$): selumetinib-*KRAS* ($p_{adj} = 4.4^{-8}$), vemurafenib-*BRAF* ($p_{adj} = 4.4^{-8}$), and dabrafenib-*BRAF* ($p_{adj} = 7.7^{-5}$). Dabrafenib-*BRAF* ($p_{adj} = 8.6^{-11}$) and trametinib-*BRAF* ($p_{adj} = 4.2^{-6}$) were significant in GDSC ($p_k = 2.3^{-3}$).

(???) Describe why we compare all pairwise combos rather than filtering for just the drug-gene combos in G2P?

To test for potentially novel drug-gene associations, we conducted similar Wilcoxon rank-sum tests for all pairwise combinations of G2P genes and drugs tested in the three drug screens (*Figures 1B and 2A*). At an unadjusted $\alpha = 0.05$, the tests revealed that in CCLE, AUC significantly correlated with mutation status for 18 out of 170 (10.59%) tested drug-gene combinations were significantly different, 135 out of 918 (14.71%) were significantly different for CTRP, and 89 out of 850 (10.47%) for GDSC.

Controlling for a FDR $< 5\%$, selumetinib-*BRAF* ($p_{adj} = 1.4^{-10}$) was the only significant drug-gene combination tested in CCLE ($p_k = 7.9^{-4}$). CTRP ($p_k = 6.5^{-4}$) yielded 5 significant combinations, one of which was selumetinib-*BRAF*. There were 3 significant G2P associations in the GDSC dataset ($p_k = 9.5^{-5}$). Of all the significant correlations between mutation status and AUC across datasets, the only genes represented were *KRAS* and *BRAF* (Figure 1). Of the 7 significant drug-gene associations across datasets, 4 were G2P associations. The remaining 3 associations were selumetinib-*BRAF*, trametinib-*KRAS*, and pazopanib-*BRAF*.

(???) Trametinib and selumetinib are both *MEK* inhibitors, and pazopanib is a *VEGFR* inhibitor. VEGF signaling can influence the MAPK/ERK signaling pathway, which promotes cell proliferation and survival. This pathway includes *RAS*, *BRAF*, and *MEK* proteins.

However, taking these results as a whole, we observe little concordance between G2P associations and the correlation of mutation status and AUC for said G2P association, suggesting that mutation status alone is not a robust predictor of clinically actionable genetic targets. This led us to examine the correlations between AUC and gene expression and AUC and copy number, two other genomic features that are known to associate with cancer and drug response. We computed Spearman correlation coefficients (r_s) between AUC of each drug-gene association and gene expression (RPKM) and copy number (\log_2 ratio) of the gene in the association. . . (???) **need to complete this thought/analysis**

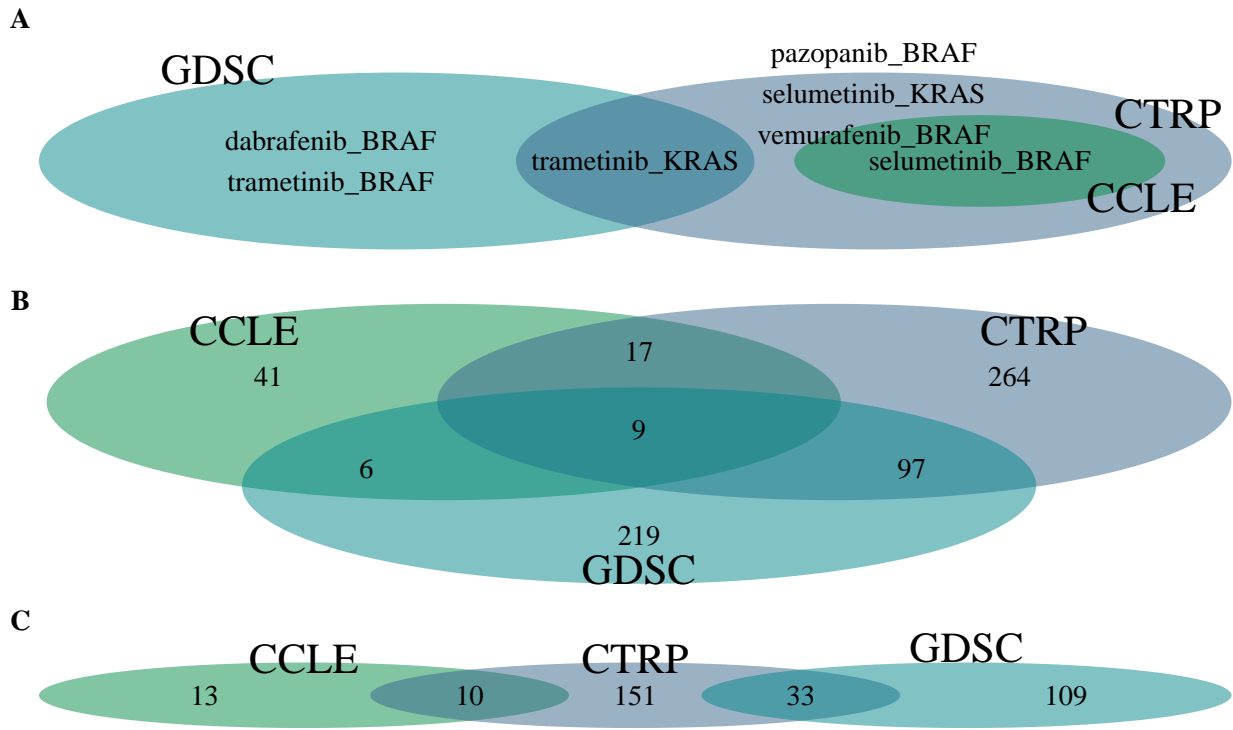


Figure 1. Overlap of drug-gene associations drawn from all pairwise combinations of G2P drugs and G2P genes whose drug effects significantly correlated with (A) mutation status, (B) gene expression, and (C) copy number across CCLE, CTRP, and GDSC.

(???) **Cut these next three paragraphs since we cut the analysis, but keep for future reference**

We compared the distribution of level-A G2P associations (*Figure 1A*) and the associated p-values from the mutation status comparisons (*Figure 1B*) with a null distribution of p-values derived from all pairwise combinations of G2P genes and the G2P drugs tested in each dataset, less any of the 88 distinct combinations with G2P interpretations, i.e. the non-gray squares in the right heatmap of *Figure 1A* (*Figure 3A*). To formally test concordance between clinically actionable variants and drug screen results, we conducted an independent, two-group t-test to compare the distributions of p-values of drug-gene combinations that either were or were not represented with level-A evidence in G2P, which indicated that the distributions of p-values did not significantly differ for CCLE [$t(9) = 0.25$, $p = 0.81$], CTRP [$t(51) = 0.85$, $p = 0.40$], nor GDSC [$t(47) = -0.56$, $p = 0.58$] (Table 2). This further supports that mutation status is not a robust genomic feature for predicting therapeutic responses.

Similar tests were conducted for the distributions of Pearson correlation coefficients (r) between the number of level-A G2P associations and gene expression (RPKM) and copy number (log2 ratio) of the gene in the association (*Figures 3B-C*). Example r derivations are shown in *Figures 2B-C*. Absolute values of r were used to simplify extreme values in both directions for testing. The difference in the CCLE $|r|$ distributions for both gene expression [$t(8) = 1.43$, $p = 0.19$] and copy number [$t(8) = 2.48$, $p = 0.23$] were non-significant, which is likely explained by the small sample size since only five G2P drugs were screened in the CCLE dataset. For both the CTRP and GDSC screens, $|r|$ values for gene expression correlations were significantly greater for the level-A G2P associations than the null distribution [$t_{\text{CTRP}}(49) = 3.79$, $p_{\text{CTRP}} < 0.001$; $t_{\text{GDSC}}(44) = 2.97$, $p_{\text{GDSC}} = 0.005$]. The $|r|$ distributions using copy number were also significantly different for CTRP [$t(49) = 2.48$, $p = 0.017$] but not for GDSC [$t(44) = 1.95$, $p = 0.058$].

In all three datasets for both level-A G2P associations and null distribution associations, there are more significant $|r|$ values when using gene expression as the genomic feature than when using copy number (Table 2), which corresponds with previous

work showing that gene expression is an informative molecular feature when assessing drug sensitivity (Jang et al., 2014; Sirota et al., 2011). Additionally, in all cases, there are more significant r values when using copy number than there are significant p -values from the mutation status comparisons. Though observational, these results suggest an order of predictive robustness for these three genomic features when used in isolation: Gene expression $>$ copy number $>$ mutation status. Additionally, across all three genomic features, CTRP consistently identified a higher percentage of its possible level-A G2P associations than GDSC, and similarly, GDSC identified a higher percentage than CCLE. In the CCLE-GDSC debate, inconsistency between the datasets was attributed to the groups using two very different assays for generating AUC measurements though it was undecided which was more accurate (Haibe-Kains et al., 2013; Jang et al., 2014; Weinstein & Lorenzi, 2013). Our results provide very preliminary evidence that GDSC is more accurate than CCLE in regards to reproducing clinical associations. However, CTRP may be even more accurate than both GDSC and CCLE.

Do these pancancer drug-gene associations penetrate to the lineage-specific level?

- What do these correlations with mutation status, gene expression, and copy number look like when you constrict to a specific lineage?
- When you restrict, do the correlations become more distinct?
- Are the lineage-specific results approximately the same as the pancancer results?
- Looking at a histogram of p -values, if the histogram is flat, then nothing is significant (note from meeting on 11/16)
- KS test results

In the 894 level-A G2P interpretations, there was a wide variation in the specificity of cancer description, ranging from “Waldenström macroglobulinemia” and “hyper

eosinophilic advanced syndrome” on the more detailed end to “cancer” on the broad end. Similarly, the drug screen datasets had a wide range in lineage specificity, e.g. CCLE, GTRP, and GDSC all had lineages labeled “leukemia” and “T-cell childhood acute lymphocytic leukemia” and the CRISPR dataset had cell lines labeled “Epstein-Barr virus-related Burkitt lymphoma” and “lymphoma.” To more easily conduct comparative analyses in a cancer-specific manner, we developed a more general lineage grouping method derived from the Human Disease Ontology identity codes (DOIDs, <http://disease-ontology.org/>) (Schriml et al., 2019) assigned to each cell line, yielding 27 unique lineage groupings. This custom lineage grouping was included in our harmonized cancer cell line database (see Methods).

In the level-A G2P interpretations, there were 102 unique drug-gene-lineage combinations (DGLs), representing seven of our curated cancer lineages: cancer, lung cancer, breast cancer, leukemia, thyroid cancer, skin cancer, and ovarian cancer. CCLE had data for 9 DGLs, CTRP had data for 61, and GDSC had data for 53, yielding a total of 73 unique DGLs across all three datasets. Only 7 DGLs were screened in all three datasets.

Prior to correction for an FDR of 5%, no DGLs were identified in the CCLE screen when using mutation status as a correlate ($n = 7$, 2 DGLs were not analyzed due to lack of mutation annotations in *UGT1A1* in “cancer” lineages), but CTRP ($n = 48$) and GDSC ($n = 39$) identified 6 and 5, respectively, in skin cancer, lung cancer, and cancer. After Benjamini-Hochberg FDR correction, none of the datasets yielded significant DGL interactions.

(???) KS test results

(Figure 2)

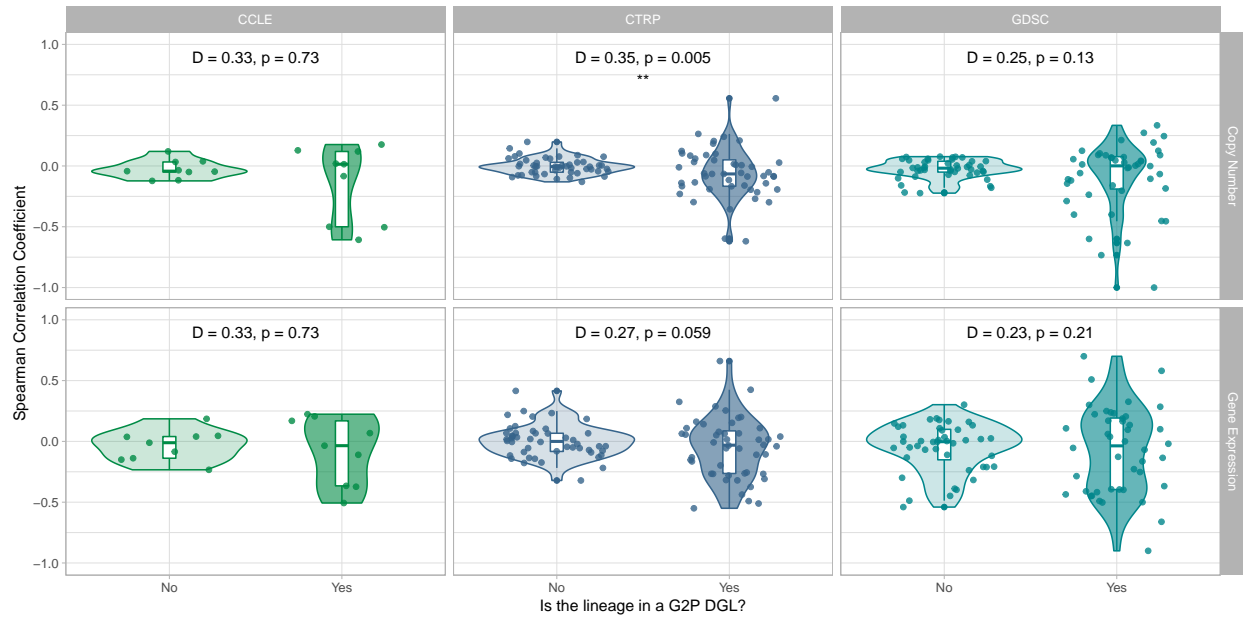


Figure 2. Comparison of Spearman correlation coefficients (r_s) derived from copy number (\log_2 ratio), gene expression (RPKM), and AUC z-scores from G2P drug-gene associations. Coefficients were grouped by whether or not the associated lineage for each comparison was in a G2P drug-gene-lineage association or not. Distributions of these grouped coefficients were compared using Kolmogorov-Smirnov tests.

Are CRISPR/Cas9 gene essentiality results comparable to those of functional drug screens?

The CRISPR screen from the Broad Institute reports gene dependency using CERES scores (Meyers et al., 2017), which are generated from sgRNA depletion scores and eliminate bias arising from the effect of copy number variation on Cas9 DNA cleavage. The lower the CERES score, the higher the likelihood that the gene is essential in the associated cell line. Scores are scaled per cell line such that a score of 0 is the median effect of nonessential genes and -1 is the median effect of common core essential genes. Of the 34 G2P genes, only *G6PD* was not targeted by an sgRNA in the CRISPR dataset.

When we don't account for lineage, Wilcoxon rank-sum tests ($p_k = 5.1^{-3}$, FDR <

5%) revealed that mutations in 2 genes significantly correlated with CERES score: *KRAS* ($p_{adj} = 2.6^{-37}$) and *BRAF* ($p_{adj} = 8.2^{-18}$). Gene expression (RPKM) of 12 out of 33 (36.36%) G2P genes significantly correlated with CERES score, as did copy number (log2-ratio) for 12 out of 33 (36.36%) G2P genes (Figure 3).

For the purpose of comparison to the drug screen data, if we treat CRISPR knockdown like a small-molecule drug, then these results are more comprehensive than the results from CCLE, CTRP, and GDSC (Table 2).

- Lineage?

Are known copy number driven associations recapitulated in the drug and CRISPR screens?

If a gene's response to is copy number driven, we would expect copy number to significantly correlate with AUC and gene essentiality scores, as would gene expression if expression and copy number are associated.

In a lineage-agnostic context of the CRISPR screen, ERBB2 gene essentiality score had a significant negative correlation with ERBB2 gene expression ($p < 10^{-12}$, $r = -0.31$) and ERBB2 copy number ($p < 10^{-15}$, $r = -0.34$) (Figure ##2). Similarly, MET gene essentiality also correlated with both MET gene expression ($p < 10^{-12}$, $r = -0.31$) and copy number ($p < 10^{-8}$, $r = -0.25$). Notably, BRCA1 also significantly correlated with both gene expression ($p < 0.001$, $r = 0.16$) and copy number ($p < 0.01$, $r = 0.14$). BRCA2 significantly correlated with all three of the genomic features tested: gene expression ($p < 0.05$, $r = 0.10$), copy number ($p < 10^{-7}$, $r = 0.23$), and mutation status ($p < 0.001$).

Which genomic features drive KRAS, EGFR, and BRAF drug-gene associations?

Should we do this?

Discussion

Level-A G2P interpretations correspond to clinical evidence that suggests efficacy of gene targets and/or drugs, and this work questions whether these relationships manifest themselves in in vitro drug screens. We have demonstrated that on its own, mutation status is not a robust predictor of drug efficacy and that copy number and gene expression fare better as predictors. However, for these three genomic features in all three datasets, only 11.1% (mutation status, 1 of 9, CCLE) to 47.9% (gene expression, 23 of 48, CTRP) (Table 2), of the level-A G2P drug-gene associations in the respective dataset were significant at an uncorrected $\alpha = 0.05$. This suggests that while the drug screens successfully identify some clinically relevant drug-gene associations, many associations are also missed, which raises the question of the extent to which clinical researchers can rely on in vitro drug screens when attempting to develop and select therapeutics for cancer patients.

These results also highlight the need to account for the complex differences inherent between data generated in clinical scenarios and data captured in highly controlled, artificial in vitro environments. Potential sources of variation and error include the fact that cells growing in a laboratory as opposed to those, even of the same tissue type, growing in a multicellular organism are exposed to differing sets of stressors and signals that can significantly impact intracellular signaling pathways, irrespective of shared genomic profiles. These differences can include, but are not be limited to, immunologic reactions, both adaptive and intrinsic (e.g. cytokine signaling, inflammation), endocrine (e.g. stress hormones), and nervous system stimulation, all of which can have significant downstream implications on cellular behavior in the context of therapeutic efficacy. Similarly, a laboratory environment and in vitro cell culture introduce abnormal growth conditions with respect to extracellular matrix composition, nutrient availability, and cell density, all of which have the potential to alter cellular signaling and thus render a drug ineffective during screening despite would-be in vivo activity.

In the era of precision medicine, the ultimate boon would be that the unique omics signatures of a patient's individual cancer can be used to guide treatment. High-throughput, in vitro screens of targeted cancer agents against cell lines with known omics profiles are beneficial for testing hypotheses concerning the mechanisms of action for these agents and they allow for scalability and systematic screening. However, extrapolating the potential downstream effects of inhibiting a major growth pathway (e.g. MAPK, IP-DAG) to predict the clinical prognosis and progression of a multicellular tumor mass growing in a complex environment, compounded with the cross-reacting effects of tumor genomic heterogeneity, make it a questionable statement that one can safely predict clinical consequences from suppressing a single pathway in a model system, as evidenced by our findings of fewer than half of the known clinical associations in the three drug screen datasets. The benefits of these cancer cell line models, in contrast, lie in their ability to assess the big-picture effects of these agents. In order to fully understand therapeutic drug response, a higher degree of granularity is needed. Additional effort to combine more cell line information such as gene expression, epigenetic profiles, and proteomic data with mutational profiles is essential to improving the efficacy and validity of in vitro cell line screens. Further benefit could be derived from conducting these screens in environments that are more in line with the clinical scenarios we are trying to predict. This would include things such a 3-dimensional cell culture, coculturing with stromal cells to mimic the tumor microenvironment, as well as other modalities that can attempt to better replicate in vivo environments.

As a next step to improve the informational granularity of the analysis presented here, our subsequent goal will be to assess the extent to which these drug-gene associations are specific to individual cancer cell line lineages, which are available and annotated in the data sets analyzed within this report. By evaluating how many clinically actionable associations are identified in these large-scale functional screens, we can begin to address best practices for translating discoveries from these tumor models into clinical trials.

Methods

G2P cancer variants

Cancer variants with the highest level of evidence (i.e. level A) in the Genotype to Phenotype (G2P) database were retrieved from the Variant Interpretation for Cancer Consortium (VICC) portal (https://search.cancervariants.org/#*) (A. H. Wagner et al., 2018) using a customized JSON-query script. All JSON queries were passed to the available application program interface (API) where a request was made for all drug-gene associations with level-A evidence via the G2P evidence label, i.e. `association.evidence_label`. From manual inspection using G2P's front-end Kibana interface, it was known that, at the time of the last query, 27 November 2018, there were 1,297 known level-A associations. Due to the limited request processing capabilities of the G2P JSON API, queries were batched into packets of 10 data points, for a total of 130 requests made in succession. Each returned request was processed as JSON object and searched to identify any existing key:value pairs for the following variables: evidence level, mutation, gene, chromosome, start, end, ref, alt, direction, phenotype description, phenotype family, phenotype ID, drug, drug ID, feature names, and sequence ID. For any evidence point where a given key:value pair was not found or unavailable, a value of -1 was assigned. One of the 1,297 level-A entries was irretrievable, yielding a final dataset of 1,296 level-A G2P interpretations, which were stored in a pandas data table and exported in CSV format. The VICC's methods for the harvesting and harmonizing of cancer variants is available in a GitHub repository from Oregon Health & Science University (<https://github.com/ohsu-comp-bio/g2p-aggregator>).

DepMap data retrieval and processing

CRISPR/Cas9, CCLE mutation calls, and CCLE copy number data were all retrieved from the Broad Institute's Cancer Dependency Map (DepMap) Public 18Q4 release via the

DepMap data portal (<https://depmap.org/portal/download/>) (Broad DepMap, 2018). Gene expression data was retrieved from the DepMap Public 18Q3 release (Broad DepMap, 2018) from the same data portal. For cell lines with no CCLE annotation, the DepMap group drew raw copy number and mutation data from whole exome sequencing data produced by the Wellcome Trust Sanger Institute [Catalogue Of Somatic Mutations In Cancer (COSMIC, https://cancer.sanger.ac.uk/cell_lines) (S. Bamford et al., 2004; S. A. Forbes et al., 2017); European Genome-phenome Archive (Lappalainen et al., 2015), accession number EGAD00001001039] and processed the data following the CCLE pipelines to ensure consistency.

CRISPR/Cas9 screen. Gene effect scores for 17,634 genes in 517 cell lines were inferred from a CRISPR/Cas9 (clustered regularly interspaced short palindromic repeats/CRISPR-associated 9) screen using the Broad Institute’s Avana knockout library (Doench et al., 2016). The Broad Institute’s data processing and screening methods are available from the figshare record (Broad DepMap, 2018) and the original publication of CERES, the algorithm that computes inferred gene dependency scores (Meyers et al., 2017). The DepMap releases new data quarterly, with the current data set being the 18Q4 release. This release has 175 more cell lines than the original data release that was published with CERES (dataset: `gene_effect.csv`, accessed 15 November 2018).

Mutation calls. To preclude variation in genomic feature calls across the datasets, we used identical annotations from CCLE for all cell lines screened in the three datasets. The CCLE provided mutation annotations in 19,280 genes across 1,596 cell lines (dataset: `depmap_18Q4_mutation_calls.csv`, accessed 14 November 2018). CCLE called substitutions using MuTect (Cibulskis et al., 2013) and annotated variants using Oncotator (Ramos et al., 2015) and indels using Indelocator (<https://software.broadinstitute.org/cancer/cga/indelocator>). We filtered mutation calls for point mutations, defined as single-nucleotide insertions, deletions, and substitutions, regardless of result, i.e. frameshift, missense, or nonsense mutation. For this analysis, cell

lines harboring non-silent point mutations were considered “mutant” for the gene in question. All other mutations and genes without annotation in the Mutation Annotation Format (MAF) file were considered “wildtype.” “Mutant” and “wildtype” calls were binarily encoded per-gene/per-cell line, regardless of quantity of harbored mutations per gene in a given cell line.

Copy number data. The CCLE generated genomic copy number (CN) data using the Affymetrix Genome-Wide Human SNP Array 6.0 and GenePattern pipeline (The Cancer Genome Atlas Research Network, 2008) and normalized segmented CN log2-ratios for 23,299 genes across 1,098 cell lines using circular binary segmentation (Olshen, Venkatraman, Lucito, & Wigler, 2004) (dataset: public_18Q4_gene_cn.csv, accessed 15 November 2018).

Gene expression data. The CCLE reports gene expression in RPKM (reads per kilobase per million mapped reads) for 54,356 genes across 1,156 cell lines, generated on the GeneChip Human Genome U133 Plus 2.0 Array (dataset: CCLE_DepMap_18q3_RNAseq_RPKM_20180718.gct, accessed 18 July 2018).

Drug screen dataset retrieval and harmonization

The Cancer Therapeutics Response Portal (CTRP) drug screen dataset (v2) (Basu et al., 2013; M. G. Rees et al., 2016; B. Seashore-Ludlow et al., 2015) was retrieved from the National Cancer Institute’s Cancer Target Discovery and Development (CTD2) Network’s data portal (<https://ocg.cancer.gov/programs/ctd2/data-portal>, accessed 6 June 2018). The Genomics of Drug Sensitivity in Cancer (GDSC) drug screen dataset (Garnett et al., 2012; Yang et al., 2012) was retrieved from the data portal at (<https://www.cancerrxgene.org/downloads>, accessed 19 June 2018). The Cancer Cell Line Encyclopedia (CCLE) drug screen dataset (J. Barretina et al., 2012; T. C. C. L. E. Consortium & Consortium, 2015) was retrieved from the Broad Institute’s data portal (<https://portals.broadinstitute.org/ccle>, accessed 20 June 2018).

Cell line harmonization. In an effort to compare CCLE, CTRP, GDSC and CRISPR results and include lineage specificity, it was necessary to consolidate cell lines screened in each dataset. Given that unique identifiers can be used between studies, it was necessary to standardize the identity of each cell line with a common source. To achieve this, a freely available cell line database called Cellosaurus (v26.0, 14 May 2018) (Bairoch, 2018) was downloaded and merged with the Broad Institute’s DepMap cell line data (accessed 8 June 2018) to create a harmonized cancer cell line database containing synonymous identifiers that enabled consolidation of all cell lines used in CCLE, CTRP, GDSC and CRISPR into a common framework. Subsequent additions to this database include the merging of DepMap IDs used in the 18Q3 and 18Q4 DepMap data releases. We curated missing synonyms and identifiers, and we manually annotated the granularity of lineage labeling for all cell lines analyzed in this study based on their Human Disease Ontology identity codes (DOIDs, <http://disease-ontology.org/>) (Schriml et al., 2019), resulting in 27 unique lineages. For ease of comparison between datasets, we labeled all cell lines with custom, randomized identifiers.

AUC harmonization. The CCLE reports cell line sensitivity to small molecules as an activity area measured above the dose-response curve (ActArea), while both CTRP and GDSC report small molecule activity as area under the dose-response curve (AUC). Since ActArea is reported with a scale of 0 to 8, we converted CCLE’s ActArea values to AUC via

$$AUC = 1 - \frac{ActArea}{8}$$

All AUC values across the three drug screen datasets were z-score transformed:

$$z = \frac{AUC - \mu_{AUC}}{\sigma_{AUC}}$$

where AUC is the mean AUC across all drug-cell line combinations in the dataset and AUC is the standard deviation.

Computational

For *Figure 1*, all data were imported and manipulated using pandas (v0.23.0) (McKinney, 2011) and plotted using seaborn (v0.90) (Waskom, 2012), which sat on top of matplotlib (v2.2.2) (Hunter, 2007) and was executed on Python (v2.7.15) (Python Software Foundation, <https://www.python.org/>) in an IPython (v5.5.0) (Pérez & Granger, 2007) kernel within a localhost Jupyter (v5.2.2) notebook (Kluyver et al., 2016). All other analyses were conducted in R (v3.5.0) (R Development Core Team, 2010, <https://www.R-project.org/>) in an RStudio environment (v1.1.447) (RStudio, 2012). All other plots were drawn using the ggplot2 (v3.0.0) R package (Wickham, 2016).

Statistics. Wilcoxon tests were conducted using the `compare_means` function in the ggpubr (v0.1.7.999) R package (Kassambara, 2018). `compare_means` does Benjamini-Hochberg p-value adjustment using the `p.adjust` function from the `stats` base R package.

For computing Spearman correlation coefficients, we used the `cor.test` base R package. If there were 3 or fewer data points, then the correlation was not done and a value of NA was supplied.

References

Finally, the APA guidelines require a note at the start of the reference section that explains what an asterisk means. This note can be added at the end of the document as follows.

Alley, M. C., Scudiere, D. A., Monks, A., Hursey, M. L., Czerwinski, M. J., Fine, D. L., . . . Boyd, M. R. (1988). Feasibility of Drug Screening with Panels of Human Tumor Cell Lines Using a Microculture Tetrazolium Assay. *Cancer Research*, 48, 589–601.

Bairoch, A. (2018). The Cellosaurus, a Cell-Line Knowledge Resource. *J Biomol Tech*, 29(2), 25–38. doi:10.7171/jbt.18-2902-002

Bamford, S., Dawson, E., Forbes, S., Clements, J., Pettett, R., Dogan, A., . . . Wooster, R. (2004). The COSMIC (Catalogue of Somatic Mutations in Cancer) database and website. *British Journal of Cancer*, 91(2), 355–358. doi:10.1038/sj.bjc.6601894

Barretina, J., Caponigro, G., Stransky, N., Venkatesan, K., Margolin, A. A., Kim, S., . . . Garraway, L. A. (2012). The Cancer Cell Line Encyclopedia enables predictive modelling of anticancer drug sensitivity. *Nature*, 483(7391), 603–607. doi:10.1038/nature11003

Basu, A., Bodycombe, N. E., Cheah, J. H., Price, E. V., Liu, K., Schaefer, G. I., . . . Schreiber, S. L. (2013). An interactive resource to identify cancer genetic and lineage dependencies targeted by small molecules. *Cell*, 154, 154(5, 5), 1151, 1151–1161. doi:10.1016/j.cell.2013.08.003, 10.1016/j.cell.2013.08.003

Ben-David, U., Siranosian, B., Ha, G., Tang, H., Oren, Y., Hinohara, K., . . . Golub, T. R. (2018). Genetic and transcriptional evolution alters cancer cell line drug response. *Nature*, 560(7718), 325–330. doi:10.1038/s41586-018-0409-3

Broad DepMap. (2018, January 11). DepMap Achilles 18Q4 public. Figshare. Retrieved

from https://figshare.com/articles/DepMap_Achilles_18Q4_public/7270880

Broad DepMap. (2018, January 8). DepMap Achilles 18Q3 public. Figshare. Retrieved from https://figshare.com/articles/DepMap_Achilles_18Q3_public/6931364

Chakravarty, D., Gao, J., Phillips, S., Kundra, R., Zhang, H., Wang, J., . . . Schultz, N. (2017). OncoKB: A Precision Oncology Knowledge Base. *JCO Precision Oncology*, (1), 1–16. doi:10.1200/PO.17.00011

Cibulskis, K., Lawrence, M. S., Carter, S. L., Sivachenko, A., Jaffe, D., Sougnez, C., . . . Getz, G. (2013). Sensitive detection of somatic point mutations in impure and heterogeneous cancer samples. *Nature Biotechnology*, 31(3), 213–219. doi:10.1038/nbt.2514

Consortium, T. C. C. L. E., & Consortium, T. G. of D. S. in C. (2015). Pharmacogenomic agreement between two cancer cell line data sets. *Nature*, 528(7580), 84–87. doi:10.1038/nature15736

Doench, J. G., Fusi, N., Sullender, M., Hegde, M., Vaimberg, E. W., Donovan, K. F., . . . Root, D. E. (2016). Optimized sgRNA design to maximize activity and minimize off-target effects of CRISPR-Cas9. *Nature Biotechnology*, 34(2), 184–191. doi:10.1038/nbt.3437

Domcke, S., Sinha, R., Levine, D. A., Sander, C., & Schultz, N. (2013). Evaluating cell lines as tumour models by comparison of genomic profiles. *Nat Commun*, 4. doi:10.1038/ncomms3126

Forbes, S. A., Beare, D., Boutselakis, H., Bamford, S., Bindal, N., Tate, J., . . . Campbell, P. J. (2017). COSMIC: Somatic cancer genetics at high-resolution. *Nucleic Acids Res*, 45(D1), D777–D783. doi:10.1093/nar/gkw1121

Garnett, M. J., Edelman, E. J., Heidorn, S. J., Greenman, C. D., Dastur, A., Lau, K. W., . . . Benes, C. H. (2012). Systematic identification of genomic markers of drug

sensitivity in cancer cells. *Nature*, 483(7391), 570–575. doi:10.1038/nature11005

Geeleher, P., Cox, N. J., & Huang, R. S. (2016). Cancer biomarker discovery is improved by accounting for variability in general levels of drug sensitivity in pre-clinical models. *Genome Biology*, 17, 190. doi:10.1186/s13059-016-1050-9

Geeleher, P., Gamazon, E. R., Seoighe, C., Cox, N. J., & Huang, R. S. (2016). Consistency in large pharmacogenomic studies. *Nature*, 540(7631), E1–E2. doi:10.1038/nature19838

Greshock, J., Bachman, K. E., Degenhardt, Y. Y., Jing, J., Wen, Y. H., Eastman, S., ... Wooster, R. (2010). Molecular Target Class Is Predictive of In vitro Response Profile. *Cancer Research*, 70(9), 3677–3686. doi:10.1158/0008-5472.CAN-09-3788

Griffith, M., Spies, N. C., Krysiak, K., McMichael, J. F., Coffman, A. C., Danos, A. M., ... Griffith, O. L. (2017). CIViC is a community knowledgebase for expert crowdsourcing the clinical interpretation of variants in cancer. *Nature Genetics*, 49(2), 170–174. doi:10.1038/ng.3774

Haibe-Kains, B., El-Hachem, N., Birkbak, N. J., Jin, A. C., Beck, A. H., Aerts, H. J. W. L., & Quackenbush, J. (2013). Inconsistency in large pharmacogenomic studies. *Nature*, 504(7480), 389–393. doi:10.1038/nature12831

Hatzis, C., Bedard, P. L., Juul Birkbak, N., Beck, A. H., Aerts, H. J. W. L., Stern, D. F., ... Haibe-Kains, B. (2014). Enhancing Reproducibility in Cancer Drug Screening: How Do We Move Forward? *Cancer Res*, 74(15), 4016–4023. doi:10.1158/0008-5472.CAN-14-0725

Haverty, P. M., Lin, E., Tan, J., Yu, Y., Lam, B., Lianoglou, S., ... Bourgon, R. (2016). Reproducible pharmacogenomic profiling of cancer cell line panels. *Nature*, 533(7603), 333–337. doi:10.1038/nature17987

Heiser, L. M., Wang, N. J., Talcott, C. L., Laderoute, K. R., Knapp, M., Guan, Y., ...

Spellman, P. T. (2009). Integrated analysis of breast cancer cell lines reveals unique signaling pathways. *Genome Biol*, 10(3), R31. doi:10.1186/gb-2009-10-3-r31

Holbeck, S. L., Collins, J. M., & Doroshow, J. H. (2010). Analysis of FDA-Approved Anti-Cancer Agents in the NCI60 Panel of Human Tumor Cell Lines. *Mol Cancer Ther*, 9(5), 1451–1460. doi:10.1158/1535-7163.MCT-10-0106

Huang, L., Fernandes, H., Zia, H., Tavassoli, P., Rennert, H., Pisapia, D., . . . Elemento, O. (2016). The cancer precision medicine knowledge base for structured clinical-grade mutations and interpretations. *J Am Med Inform Assoc*, 24(3), 513–519. doi:10.1093/jamia/ocw148

Hunter, J. (2007). Matplotlib: A 2D graphics environment, 9(3), 90–95. doi:10.5281/zenodo.1202077

Jang, I. S., Neto, E. C., Guinney, J., Friend, S. H., & Margolin, A. A. (2014). Systematic assessment of analytical methods for drug sensitivity prediction from cancer cell line data. *Pac Symp Biocomput*, 63–74. Retrieved from <https://www.ncbi.nlm.nih.gov/pmc/articles/PMC3995541/>

Kassambara, A. (2018). Ggpubr: 'Ggplot2' Based Publication Ready Plots (Version 0.1.7.999). Retrieved from <https://cran.r-project.org/web/packages/ggpubr/index.html>

Kluyver, T., Ragan-Kelley, B., Pérez, F., Granger, B., Bussonnier, M., Frederic, J., . . . Team, J. D. (2016). Jupyter Notebooks - a publishing format for reproducible computational workflows. In F. Loizides & B. Schmidt (Eds.), *Positioning and Power in Academic Publishing: Players, Agents and Agendas* (pp. 87–90). IOS Press.

Lappalainen, I., Almeida-King, J., Kumanduri, V., Senf, A., Spalding, J. D., ur-Rehman, S., . . . Flicek, P. (2015). The European Genome-phenome Archive of human data

consented for biomedical research. *Nat Genet*, 47(7), 692–695. doi:10.1038/ng.3312

Marcotte, R., Brown, K. R., Suarez, F., Sayad, A., Karamboulas, K., Krzyzanowski, P. M.,
... Moffat, J. (2012). Essential gene profiles in breast, pancreas and ovarian cancer
cells. *Cancer Discov*, 2(2), 172–189. doi:10.1158/2159-8290.CD-11-0224

McDonald, E. R., de Weck, A., Schlabach, M. R., Billy, E., Mavrakis, K. J., Hoffman, G.
R., ... Sellers, W. R. (2017). Project DRIVE: A Compendium of Cancer
Dependencies and Synthetic Lethal Relationships Uncovered by Large-Scale, Deep
RNAi Screening. *Cell*, 170(3), 577–592.e10. doi:10.1016/j.cell.2017.07.005

McFarland, J. M., Ho, Z. V., Kugener, G., Dempster, J. M., Montgomery, P. G., Bryan, J.
G., ... Tsherniak, A. (2018). Improved estimation of cancer dependencies from
large-scale RNAi screens using model-based normalization and data integration.
doi:10.1101/305656

McKinney, W. (2011). Pandas: A Foundational Python Library for Data Analysis and
Statistics. Retrieved from <http://pandas.pydata.org/>

Meyers, R. M., Bryan, J. G., McFarland, J. M., Weir, B. A., Sizemore, A. E., Xu, H., ...
Tsherniak, A. (2017). Computational correction of copy-number effect improves
specificity of CRISPR-Cas9 essentiality screens in cancer cells. *Nat Genet*, 49(12),
1779–1784. doi:10.1038/ng.3984

Mouradov, D., Sloggett, C., Jorissen, R. N., Love, C. G., Li, S., Burgess, A. W., ... Sieber,
O. M. (2014). Colorectal Cancer Cell Lines Are Representative Models of the Main
Molecular Subtypes of Primary Cancer. *Cancer Research*, 74(12), 3238–3247.
doi:10.1158/0008-5472.CAN-14-0013

Neve, R. M., Chin, K., Fridlyand, J., Yeh, J., Baehner, F. L., Fevr, T., ... Gray, J. W.
(2006). A collection of breast cancer cell lines for the study of functionally distinct

cancer subtypes. *Cancer Cell*, 10(6), 515–527. doi:10.1016/j.ccr.2006.10.008

Olshen, A. B., Venkatraman, E. S., Lucito, R., & Wigler, M. (2004). Circular binary segmentation for the analysis of array-based DNA copy number data. *Biostatistics*, 5(4), 557–572. doi:10.1093/biostatistics/kxh008

Patel, S. J., Sanjana, N. E., Kishton, R. J., Eidizadeh, A., Vodnala, S. K., Cam, M., . . . Restifo, N. P. (2017). Identification of essential genes for cancer immunotherapy. *Nature*, 548(7669), 537–542. doi:10.1038/nature23477

Patterson, S. E., Liu, R., Statz, C. M., Durkin, D., Lakshminarayana, A., & Mockus, S. M. (2016). The clinical trial landscape in oncology and connectivity of somatic mutational profiles to targeted therapies. *Human Genomics*, 10(1). doi:10.1186/s40246-016-0061-7

Paz, M. F., Fraga, M. F., Avila, S., Guo, M., Pollan, M., Herman, J. G., & Esteller, M. (2003). A Systematic Profile of DNA Methylation in Human Cancer Cell Lines, 63, 1114–1121.

Pérez, F., & Granger, B. (2007). IPython: A System for Interactive Scientific Computing, 9(3), 21–29. doi:10.1109/MCSE.2007.53

R Development Core Team. (2010). *R: A Language and Environment for Statistical Computing*. Vienna, Austria: R Foundation for Statistical Computing. Retrieved from <https://www.R-project.org/>

Ramos, A. H., Lichtenstein, L., Gupta, M., Lawrence, M. S., Pugh, T. J., Saksena, G., . . . Getz, G. (2015). Oncotator: Cancer Variant Annotation Tool. *Human Mutation*, 36(4), E2423–E2429. doi:10.1002/humu.22771

Rees, M. G., Seashore-Ludlow, B., Cheah, J. H., Adams, D. J., Price, E. V., Gill, S., . . . Schreiber, S. L. (2016). Correlating chemical sensitivity and basal gene expression reveals mechanism of action. *Nat Chem Biol*, 12(2), 109–116.

doi:10.1038/nchembio.1986

RStudio. (2012). RStudio: Integrated development environment for R (Version 1.1.447).

Boston, MA: RStudio.

Safikhani, Z., El-Hachem, N., Smirnov, P., Freeman, M., Goldenberg, A., Birkbak, N. J.,
... Haibe-Kains, B. (2016). Safikhani et al. reply. *Nature*, 540(7631), E2–E4.

doi:10.1038/nature19839

Safikhani, Z., Smirnov, P., Freeman, M., El-Hachem, N., She, A., Rene, Q., ...

Haibe-Kains, B. (2017). Revisiting inconsistency in large pharmacogenomic studies.

F1000Res, 5. doi:10.12688/f1000research.9611.3

Schriml, L. M., Mitraka, E., Munro, J., Tauber, B., Schor, M., Nickle, L., ... Greene, C.

(2019). Human Disease Ontology 2018 update: Classification, content and workflow
expansion, 1–8. doi:10.1093/nar/gky1032

Seashore-Ludlow, B., Rees, M. G., Cheah, J. H., Cokol, M., Price, E. V., Coletti, M. E., ...

Schreiber, S. L. (2015). Harnessing Connectivity in a Large-Scale Small-Molecule
Sensitivity Dataset. *Cancer Discov*, 5, 5(11, 11), 1210, 1210–1223.

doi:10.1158/2159-8290.CD-15-0235, 10.1158/2159-8290.CD-15-0235

Shoemaker, R. H. (2006). The NCI60 human tumour cell line anticancer drug screen.

Nature Reviews Cancer, 6(10), 813–823. doi:10.1038/nrc1951

Sirota, M., Dudley, J. T., Kim, J., Chiang, A. P., Morgan, A. A., Sweet-Cordero, A., ...

Butte, A. J. (2011). Discovery and preclinical validation of drug indications using
compendia of public gene expression data. *Sci Transl Med*, 3(96), 96ra77.

doi:10.1126/scitranslmed.3001318

Stinson, S., Alley, M., Kopp, W., Fiebig, H., Mullendore, L., Pittman, A., ... Boyd, M.

(1992). Morphological and immunocytochemical characteristics of human tumor cell

lines for use in a disease-oriented anticancer drug screen, *12*(4), 1035–1053.

Tamborero, D., Rubio-Perez, C., Deu-Pons, J., Schroeder, M. P., Vivancos, A., Rovira, A.,
... Lopez-Bigas, N. (2018). Cancer Genome Interpreter annotates the biological
and clinical relevance of tumor alterations. *Genome Med*, *10*.
doi:10.1186/s13073-018-0531-8

The Cancer Genome Atlas Research Network. (2008). Comprehensive genomic
characterization defines human glioblastoma genes and core pathways, *455*,
1061–1068. doi:10.1038/nature07385

The Global Alliance for Genomics and Health. (2016). A federated ecosystem for sharing
genomic, clinical data. *Science*, *352*(6291), 1278–1280. doi:10.1126/science.aaf6162

Varley, K. E., Gertz, J., Bowling, K. M., Parker, S. L., Reddy, T. E., Pauli-Behn, F., ...
Myers, R. M. (2013). Dynamic DNA methylation across diverse human cell lines
and tissues. *Genome Res*, *23*(3), 555–567. doi:10.1101/gr.147942.112

Wagner, A. H., Walsh, B., Mayfield, G., Tamborero, D., Sonkin, D., Krysiak, K., ...
Margolin, A. (2018). A harmonized meta-knowledgebase of clinical interpretations
of cancer genomic variants. doi:10.1101/366856

Wang, T., Birsoy, K., Hughes, N. W., Krupczak, K. M., Post, Y., Wei, J. J., ... Sabatini,
D. M. (2015). Identification and characterization of essential genes in the human
genome. *Science*, *350*(6264), 1096–1101. doi:10.1126/science.aac7041

Waskom, M. (2012). Seaborn: Statistical data visualization (Version 0.9.0). Retrieved from
<http://seaborn.pydata.org/>

Weinstein, J. N., & Lorenzi, P. L. (2013). Discrepancies in drug sensitivity, *504*(7480),
381–313. doi:10.1038/504383a

Wickham, H. (2016). Ggplot2: Elegant Graphics for Data Analysis (Version 3.0.0).

Retrieved from <http://ggplot2.org>

- Yang, W., Soares, J., Greninger, P., Edelman, E. J., Lightfoot, H., Forbes, S., ... Garnett, M. J. (2012). Genomics of Drug Sensitivity in Cancer (GDSC): A resource for therapeutic biomarker discovery in cancer cells. *Nucleic Acids Res*, *41*(D1), D955–D961. doi:10.1093/nar/gks1111
- Yu, M., Selvaraj, S. K., Liang-Chu, M. M. Y., Aghajani, S., Busse, M., Yuan, J., ... Neve, R. M. (2015). A resource for cell line authentication, annotation and quality control. *Nature*, *520*(7547), 307–311. doi:10.1038/nature14397

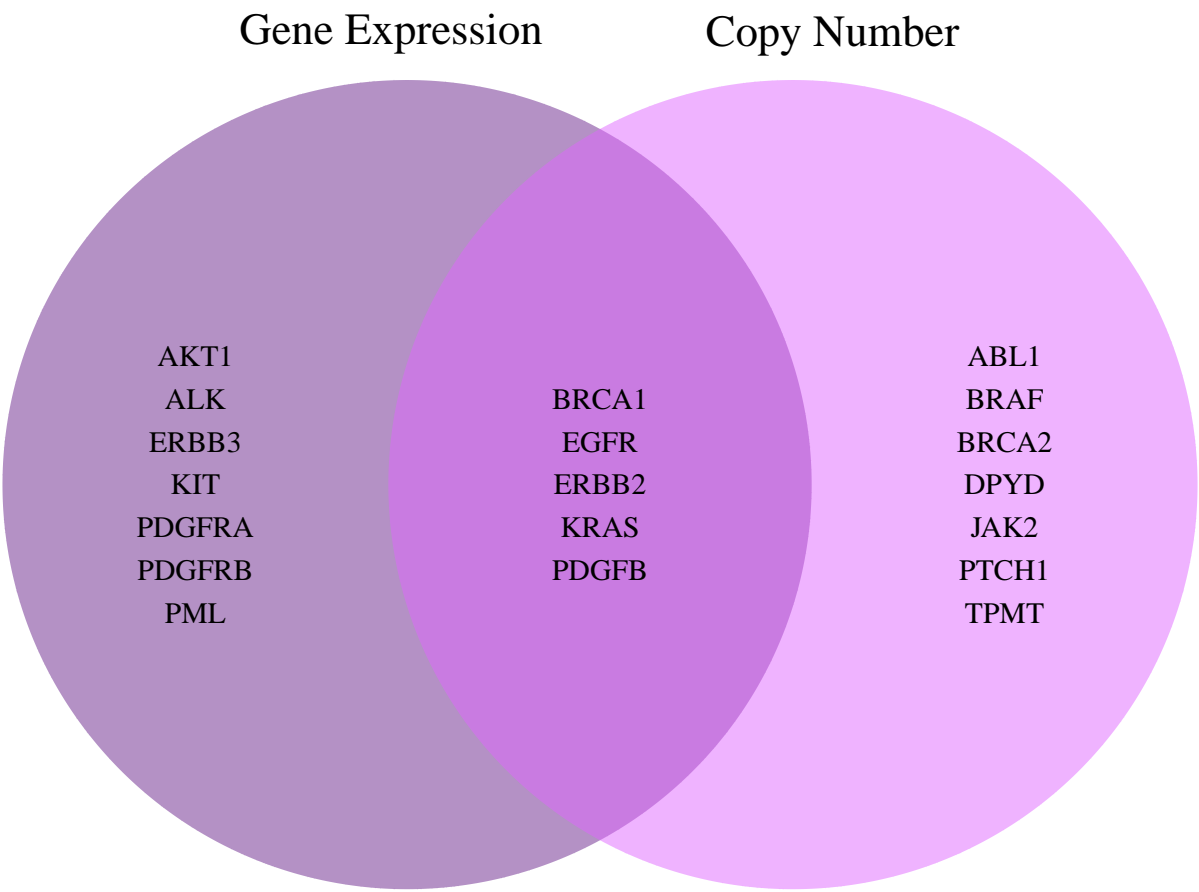


Figure 3. Overlap of genes whose gene expression and/or copy number significantly correlated with CERES score.